Hindawi
Journal of Chemistry
Volume 2019, Article ID 3017163, 11 pages
https://doi.org/10.1155/2019/3017163

Research Article

Pineapple Bark Performance in Dyes Adsorption: Optimization by the Central Composite Design

Ahlam Fegousse,[1] **Abdelali El Gaidoumi**,[2] **Youssef Miyah**,[2] **Rabea El Mountassir**,[1] **and Anissa Lahrichi**[1]

[1]*Laboratory of Biochemistry, Faculty of Medicine and Pharmacy, Sidi Mohamed Ben Abdellah University, 30000 Fez, Morocco*
[2]*Laboratory of Catalysis, Materials and Environment, Higher School Technology, Sidi Mohamed Ben Abdellah University, 30000 Fez, Morocco*

Correspondence should be addressed to Ahlam Fegousse; ahlam.fegousse@gmail.com

Received 24 November 2018; Revised 31 December 2018; Accepted 15 January 2019; Published 14 February 2019

Academic Editor: Nicolas Roche

This work is concerned with the study of the adsorption in aqueous medium of a three-dye mixture which contains Methylene Blue, Brilliant Green, and Congo Red on the pineapple bark. This adsorbent material has been characterized by scanning electron microscopy (SEM) and Fourier transform infrared spectroscopy (FTIR). The experimental design methodology, based on the response surface methodology (RSM) by the central composite design (CCD), has been applied for the optimization of the parameters, namely, the temperature, dose of the adsorbent, and pH. The yield reached 98.91% under optimal conditions ($T = 30^{\circ}C$; adsorbent dose = 2.5 $g{\cdot}L^{-1}$; pH = 9.8) at an initial concentration of 20 $mg{\cdot}L^{-1}$.

1. Introduction

Water is an essential element for the survival of all living organisms. Nowadays, the water sources contaminated by a wide variety of pollutants coming from industrial effluents are a subject of several researchers [1, 2]. Dyes have a large amount of pollutants and can be identified even by the human eye [3]. In this respect, dyes are used in various industries such as textiles, food, paper, rubber, plastics, and cosmetics [4]. Hence, the discharge of wastewater from these industries to water resources poses unavoidable problems. The presence of dyes in trace water is undesirable because most of them are toxic, mutagenic, and carcinogenic [5]. Furthermore, dyes not only prevent the penetration of light and reduce the photosynthetic activities of rivers but also disturb the aquatic balance. Thus, the elimination of dyes from wastewater before discharge is an indispensable task. In this case, several techniques such as flocculation, adsorption, oxidation, electrolysis, biodegradation, ion exchange, and photocatalysis have been used for the removal of dyes in wastewater [6]. Among the several techniques, adsorption has received considerable attention because of its many advantages in terms of cost, ease of use, flexibility and simplicity of design, and insensitivity to toxic pollutants [7, 8]. Similarly, of the various adsorbents, activated carbon may be the most effective adsorbent for the removal of dyes due to its excellent adsorption capacity [9]. However, its use is limited on account of its high cost [10]. Thus, attention has shifted to finding cheaper and more effective alternatives. For this reason, natural materials, agricultural and industrial waste, and biosorbents represent potential alternatives. Additionally, a large number of unconventional and low-cost adsorbents have been proposed by many researchers for the removal of dyes [11, 12] including agricultural waste such as sawdust [13], bark [14], and orange peel [15] and industrial waste, namely, metal hydroxide sludge [16], red mud [17], ashes flying [18], clays [19–21], diatomites [22, 23], zeolites [24, 25], siliceous materials [26, 27], biosorbents [28–31], and others (cyclodextrin [32, 33], starch [34], cotton [35], etc.).

The purpose of this work was to study the adsorption of a three-dye mixture that contained Methylene Blue, Brilliant

Green, and Congo Red on the pineapple bark according to the surface response method using the central composite design that consists of optimizing physicochemical parameters such as pH, temperature, and mass of the adsorbent.

2. Materials and Methods

2.1. Preparation of the Adsorbate and Adsorbent. The studied dyes have been supplied by Sigma-Aldrich and used without prior treatment. Congo Red (CR) is an anionic dye, part of the class of azo, with chemical formula $C_{32}H_{22}N_6O_6S_2Na_2$ and molar mass equal to 696.66 g·mol^{-1}. Its molecular structure is illustrated in Figure 1(a). Methylene Blue (MB) and Brilliant Green (BG) which are cationic dyes, with chemical formulas of $C_{16}H_{18}ClN_3S$ and $C_{27}H_{34}N_2O_4S$ and molar masses equal to 319.85 g·mol^{-1} and 482.63 g·mol^{-1}, respectively. Their molecular structures are shown schematically in Figures 1(b) and 1(c). The colored solution (DM) has been precisely prepared by mixing the three dyes with same proportion in ultrapure water.

The pineapple bark (PB) was washed with ultrapure water followed by free-air drying. After that, it was crushed and sieved to a fraction less than 125 nm. The resulting powder was then washed with ultrapure water to remove impurities and then oven-dried at a temperature of 60°C.

2.2. Adsorption Procedure. The experiments have been performed in a batch system with constant stirring in Pyrex beakers using a volume of 50 mL of colored solution. Moreover, 4 mL samples have been taken using a 0.45 μm diameter syringe filter and then analyzed by a Jasco V-750 UV-Vis spectrophotometer at a wavelength $\lambda_{max} = 624$ nm.

The capacity of adsorption was calculated according to

$$q_t = \frac{(C_0 - C_t) * V}{m}, \quad (1)$$

where q_t is the amount of adsorbed dye per unit adsorbent at instant t (mg/g), m is the used mass of adsorbent (g), C_0 is the initial concentration of dye in solution (mg/L), C_t is the concentration of dye in solution at instant t (mg/L), and V is the used volume of solution (L).

The concentrations and removal percentages were calculated taking into account the dyes' purity: ≥35%, ≥82%, and ≥90% for CR, MB, and BG, respectively.

2.3. Characterization Techniques. Morphological analysis was observed by scanning electron microscopy (SEM) using a Quanta 200 FEI microscope. Fourier transform infrared spectroscopy (FTIR) analysis was performed in the 400–4000 cm^{-1} interval using a Bruker Vertex 70 spectrometer to determine the functional analysis of the PB powder.

The point zero of charge (pH_{PZC}) was determined by a classical method [36], which consists in preparing 50 mL solutions of NaCl (0.01 M) and adjusting their pH to precise values ranging from 2 to 12 by addition of NaOH or HCl (0.1 M). Next, 0.5 g of adsorbent was introduced into each solution. The suspensions were stirred at room temperature for 24 h before determining the pH_{final}. The pH_{PZC} was calculated based on the curve $pH_{final} - pH_{initial} = f(pH_{initial})$.

3. Results and Discussions

3.1. Characterizations of the Adsorbent. The use of the SEM technique makes it possible to visualize the morphology of the surface of the adsorbent. The SEM micrographs of PB are shown in Figure 2. The obtained images display not only the amorphous nature and the heterogeneous morphology of PB but also indicate the presence of both a grainy structure (Figure 2(b)) close to the appearance of the grapes and a filamentous structure and cellulosic fibers of various sizes and shapes (Figure 2(c)), which promote the fixation of dyes. Consequently, these results are similar to those obtained by Miyah et al. [37].

FTIR spectrum analysis (Figure 3) shows a band around 3444.03 cm^{-1} which is characteristic of the presence of a band O-H group, a small band around 2925.38 cm^{-1} which attributes to C-H elongation vibrations, a band at 2361.24 cm^{-1} which could be due to the nitrile triple bond C≡N, a band at 1633.21 cm^{-1} which originates from the vibration of the C=O groups, a band at 1398.56 cm^{-1} which coincides with the OH band aromatic alcohol, a 1255.45 cm^{-1} band which corresponds to the CO bond, a 1037.19 cm^{-1} band which is assigned to the primary alcohol function (C-OH), and a band at 668.09 cm^{-1} which characterizes the function ≡CH [39].

The pH_{PZC} corresponds to the pH value for which the net electric charge of the surface of the material is neutral [40]. pH_{PZC} is very important in adsorption phenomena, especially when electrostatic forces are involved in the mechanisms. Figure 4 shows that the pH_{PZC} of PB is 6.7. This point illustrates an amphoteric behavior of PB. In fact, the surface of PB is positively charged at $pH < pH_{PZC}$ and negatively charged at $pH > pH_{PZC}$. As pH decreases, the number of negatively charged sites decreases, and the number of positively charged sites increases and vice versa when pH increases [41–43].

3.2. Effect of Contact Time. As illustrated in Figure 5, the equilibrium time is reached in the first five minutes for a concentration range varying between 20 mg·L^{-1} and 50 mg·L^{-1}. This can be explained by the fact that the available number of active sites on the surface of adsorbent becomes saturated after five minutes [44]. In this case, the adsorption capacity (Q_e) remains constant after equilibrium time, which denotes that the adsorption is rapid and confirms strong chemical interactions between the dye molecules and adsorbent. In this respect, these outcomes allow us to have a quick overview on the effectiveness of PB.

3.3. Effect of Adsorbent Dose. Figure 6(a) shows the monitoring of the adsorption capacity as a function of time at an initial concentration of 20 mg·L^{-1}; a large decrease in the DM adsorbed amount with the increase of the adsorbent dose was observed. This phenomenon is due to the decrease of number of DM molecules (decrease in concentration) and the difficulty of adsorbent-adsorbate interaction, which explains the saturation of the active sites of the adsorbent. Additionally, while the curve which is a function of the

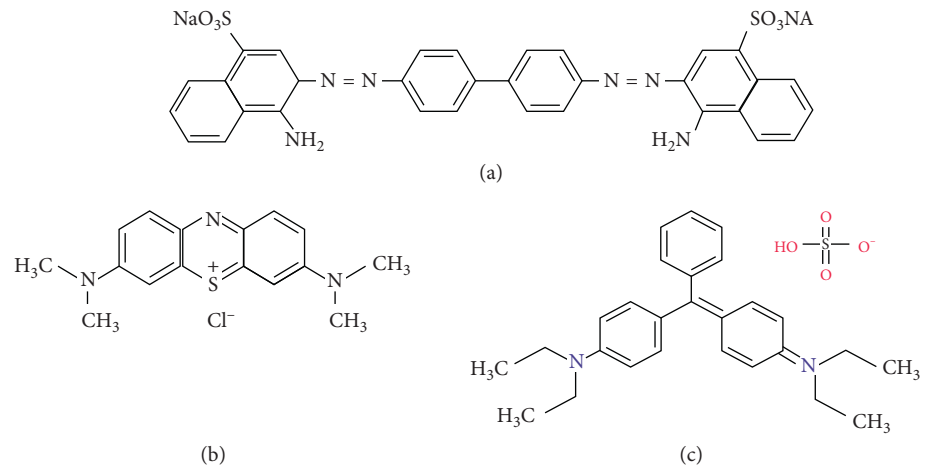

Figure 1: Chemical structure of dyes: (a) Congo Red, (b) Methylene Blue, and (c) Brilliant Green.

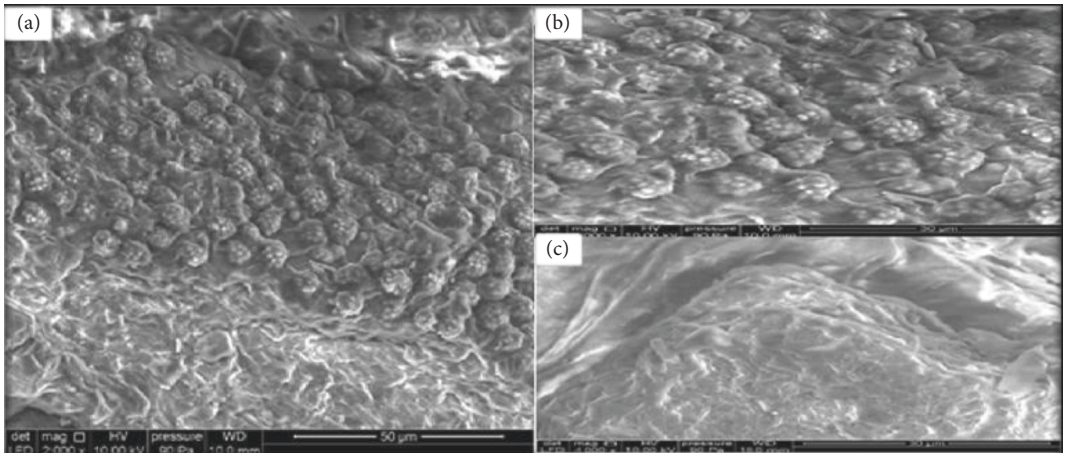

Figure 2: SEM micrographs of PB: magnification (a) ×2000; (b, c) ×4000 (reproduced from Fegousse et al. [38]).

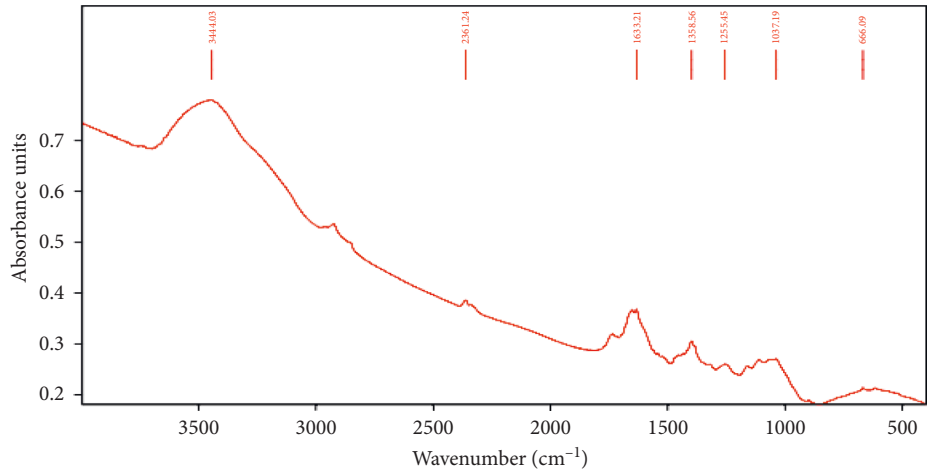

Figure 3: FTIR spectra of PB (reproduced from Fegousse et al. [38]).

adsorption efficiency (Figure 6(b)) has a proportionally inverse appearance to that of the adsorbed quantity, it is obviously noticed that the adsorption efficiency increases with the increase in the adsorbent dose. Hence, 2 g·L^{-1} of the adsorbent constitutes an optimal dose to remove 97.93% of DM which corresponds to an adsorption capacity of 14.6 mg·g^{-1}.

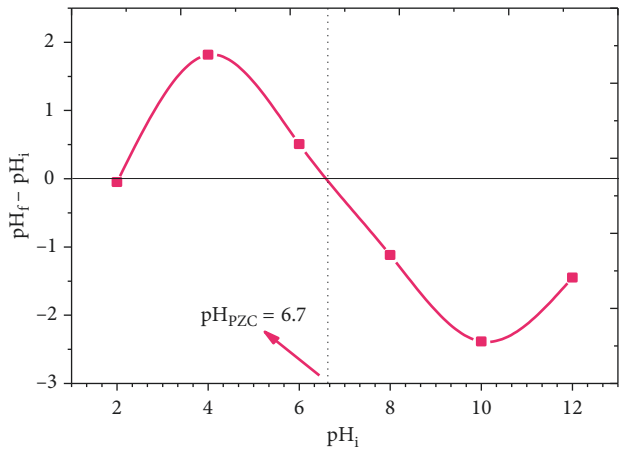

Figure 4: The point zero of charge of PB.

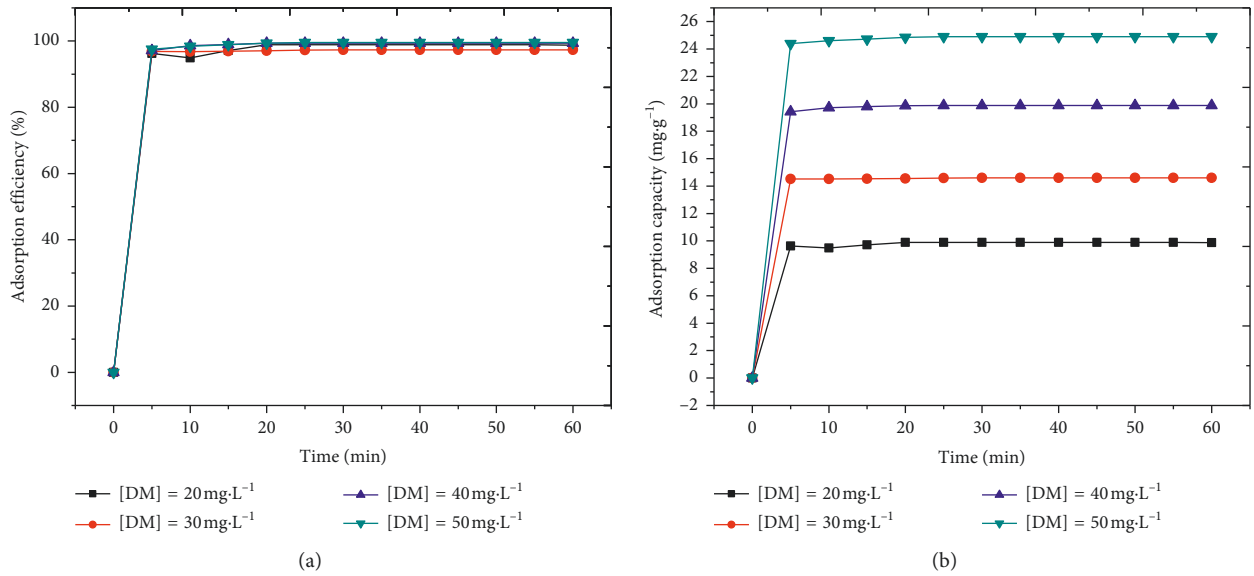

Figure 5: Effect of contact time on (a) adsorption efficiency and (b) adsorption capacity at different concentrations. $m = 2.\text{g}\cdot\text{L}^{-1}$; [DM] = 20–50 mg·L^{-1}; $T = 20^{\circ}\text{C}$, pH = 6; $V_{ag} = 400$ rpm; $t = 60$ min.

3.4. Effect of Temperature. The outcomes of the evolution of the adsorption capacity as a function of temperature at an initial concentration of 20 mg·L^{-1} are displayed in Figure 7. In this respect, the analysis of the curve shows that the temperature has a negative effect on the adsorption capacity; it affects the chemical potential of the material: the mobility of the system increases but the interactions decrease. This suggests that the interaction of PB and DM may be exothermic. Thus, the adsorption capacity reaches 9.87 mg·g^{-1} for a temperature of 20°C which corresponds to a removal efficiency of 98.97%.

The adsorption may result in decreasing or increasing the surface energy of the adsorbent materials. The parameters that can describe the adsorption thermodynamics due to the transfer of the solute to the solid-liquid interface are the standard enthalpy (ΔH°), the standard entropy (ΔS°), and the free standard enthalpy (ΔG°). The values of ΔH° and ΔS° were calculated using equation (2) [4] by plotting $\ln K_d$ as a function of $1/T$ (Figure 8).

$$\ln K_d = \frac{\Delta S^{\circ}}{R} - \frac{\Delta H^{\circ}}{RT}, \tag{2}$$

where R is the ideal gas constant ($R = 8.314\ \text{J}\cdot\text{mol}^{-1}\cdot\text{K}^{-1}$); T is the absolute temperature of solution (K); and K_d is the distribution coefficient equal to Q_e/C_e (Q_e and C_e represent the capacity of adsorption and concentration at equilibrium, respectively).

The values of ΔG° were calculated using the following formula [4]:

$$\Delta G^{\circ} = -RT \ln K_d. \tag{3}$$

The obtained results show that the standard enthalpy value is negative (Table 1), which confirms that the adsorption of the dye molecules at the sites of the PB adsorbent

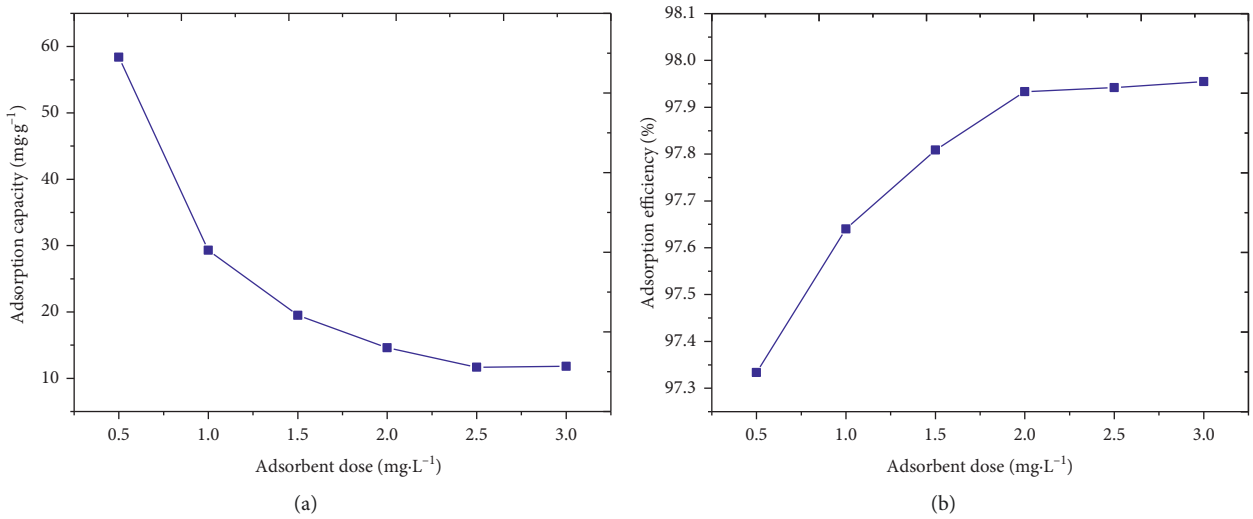

FIGURE 6: Effect of PB dose on (a) adsorption capacity and (b) adsorption efficiency. $m = 0.5$–$3\ \text{g·L}^{-1}$; [DM] $= 20\ \text{mg·L}^{-1}$; $T = 20^{\circ}\text{C}$; pH = 6; $V_{ag} = 400$ rpm; $t = 60$ min.

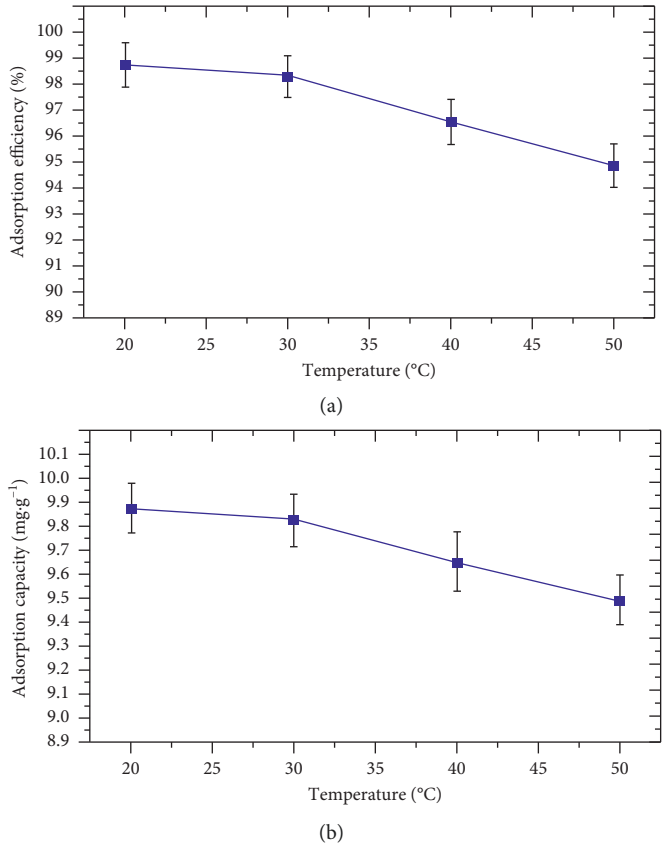

FIGURE 7: Effect of temperature on (a) adsorption efficiency and (b) adsorption capacity. $m = 2\ \text{g·L}^{-1}$; [DM] $= 20\ \text{mg·L}^{-1}$; $T = 20$–50°C; pH = 6; $V_{ag} = 400$ rpm; $t = 60$ min.

is exothermic. The negative values of the free standard enthalpy and standard entropy indicate that the process of adsorption of the DM on PB is spontaneous and follows a disorder, respectively.

3.5. Effect of pH. The evolution of DM adsorption as a function of pH at an initial concentration of $20\ \text{mg·L}^{-1}$ and dose of $2\ \text{g·L}^{-1}$ is illustrated in Figure 9. The adsorption is favorable at acid pH due to the positive charge of the

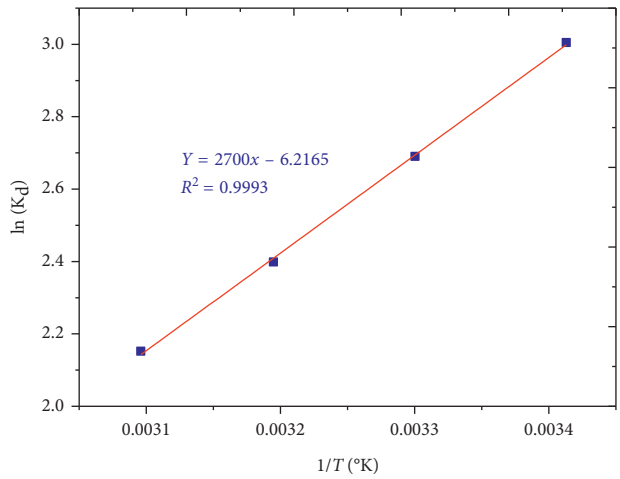

Figure 8: $\ln K_d$ versus $1/T$ for the adsorption of DM on PB.

Table 1: Thermodynamic parameters of the adsorption process of DM on PB.

Temperature (°C)	ΔH° (KJ·mol^{-1})	ΔS° (J·mol^{-1}·K^{-1})	ΔG° (J·mol^{-1})	R^2
20	−22.44	−51.68	−37591.20	0.9993
30			−38108.04	
40			−38624.88	
50			−39141.72	

adsorbent which promotes the adsorption of the negatively charged anionic dye (RC). On the contrary, at basic pH, the adsorption is stable even in the presence of cationic dyes (MB and BG). This indicates that the adsorbent is selective for the anionic dye and only at acidic pH. Furthermore, the adsorption of the cationic dyes is owing to the activation of the surface of the adsorbent by the anionic dye which makes the surface negative and, therefore, active in front of the cationic dyes. Indeed, for acid pH values, the cationic dyes are in competition with the H^+ ions presented in high concentration in the solution [45,46]. These ions, positively charged, are more adsorbed than cationic dyes and then beneficial for adsorption of anionic dye with negative charge. Additionally, when the pH increases, there is a decrease in the H^+ ions and increase in OH^-, which explains the favorability of the adsorbent to absorb the cationic dyes. Based on the obtained results, pH = 6 is the optimum value for the adsorption of DM.

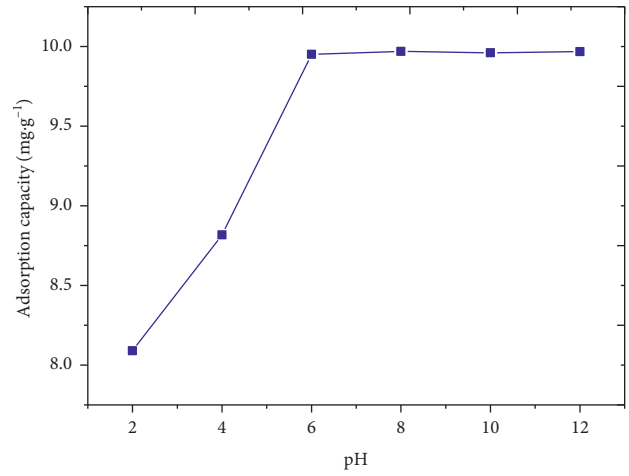

Figure 9: pH effect on PB adsorption capacity. $m = 2$ g·L^{-1}; [DM] = 20 mg·L^{-1}; $T = 20$°C; pH = 2–12; $V_{ag} = 400$ rpm; $t = 30$ min.

3.6. Optimization of Adsorption. The aim of this study is to optimize the adsorption of the mixture of dyes by the response surface methodology (RSM). The design used for the optimization, belonging to RSM, is the central composite design (CCD); its equation is polynomial of second order [47]:

$$Y_i = b_0 + b_1X_1 + b_2X_2 + b_3X_3 + b_{12}X_1X_2 + b_{13}X_1X_3 + b_{23}X_2X_3 + b_{11}X_1^2 + b_{22}X_2^2 + b_{33}X_3^2, \quad (4)$$

where Y represents the percentage of adsorption, X_i represents the independent variable (temperature, pH or dose of the adsorbent), X_iX_j demonstrates the interactions between the variables, and b_i represents the coefficient of the effect resulted by X_i.

The number of experiments to be performed is determined by the following formula:

$$N = 2^K + 2K + f, \quad (5)$$

where K is the number of independent variables and f is the number of experiments performed at the center of the experimental scope.

To realize 17 experiments according to the computation of the formula (3), each variable is represented by 5 levels: −1.68; −1; 0; +1; 1.68.

3.7. Table of Variables. Table 2 represents the three studied variables and their corresponding levels. The reaction time is 5 min, and the concentration of DM was fixed at 20 mg·L^{-1}.

3.8. Experimental Matrix and Postulated Mathematical Model. Table 3 summarizes the 17 performed experiments according to the CCD design. Experiments 15, 16, and 17 represent the experiments at the center. According to the results, the percentage of adsorption varies between 75.55% and 97.18%. The mathematical model generated by the Design-Expert software version 11 is

$$Y = 97.22 + 1.83X_1 + 7.22X_2 + 1.77X_3 - 2.95X_1^2 - 3.35X_2^2 - 1.43X_3^2 + 0.52X_1X_2 + 1.77X_1X_3 - 3.56X_2X_3. \quad (6)$$

3.9. ANOVA Analysis. Analysis of variance (ANOVA) has been used, and the results are given in Table 4. Generally, the adaptation of the postulated model is confirmed by a high Fisher value (F) with as low a probability (P) as possible. From the ANOVA test, the obtained P value of 0.0001 is less than 0.05 value evaluated by the Fischer relation which confirms that the model terms are significant [48,49]. The resulting F value of 230.5 is greater than the Fisher value of $F_{9.7} = 3.8$ for a 95% confidence level. So, the model is well suited to experimental data [50–52].

The fit quality of the model can be justified by the correlation coefficient (R^2) which indicates the proportion of the response variability taken into account by the model [53]. The best correlation is obtained for which $R^2 = 0.80$ is suggested [54]. The obtained R value of 0.9966 (Table 5) implied that a large proportion of the variability of the response is considered by the model; 0.34% of the variations are not taken into account.

3.10. Estimation of Coefficients. The determination of the coefficients makes it possible to judge the significance of the effects of the variables and their interactions. Thus, Table 6 summarizes the results found.

Generally, interaction coefficients that have a P value less than 0.05 consider themselves as coefficients having a significant effect on the response. According to the previous table, all P values are less than 0.05; so, all coefficients are considered to have a very crucial effect on the response, except in the case of b_{11} for which P is equal to 0.0847.

3.11. Graphic Study. The graphical representations of three response surfaces are illustrated in Figure 10. In this respect, the optimum point of the adsorption yield has been achieved based on the response surface of the X_2X_3, interaction between pH and adsorbent dose (Figure 10(c)), which have already shown a positive effect on yield (Figures 6 and 9). Besides, the maximum yield that is not acquired according to the X_1X_2 and X_1X_3 interactions (Figures 10(a) and 10(b)) is justified by the negative effect of temperature (X_1) on the adsorption process (Figure 7). Hence, the optimal conditions are summarized in Table 7.

Table 2: Description of the variables and their levels.

Parameters	Variables	Levels				
		−1.68	−1	0	+1	+1.68
T (°C)	X_1	20	30	40	50	60
pH	X_2	2	4	6	8	10
m (adsorbent dose) (g·L^{-1})	X_3	0.5	1	1.5	2	2.5

Table 3: Experimental matrix.

Experience	Variables			Response
	X_1	X_2	X_3	Y
1	−1	−1	−1	77.01
2	1	−1	−1	76.81
3	−1	1	−1	98.75
4	1	1	−1	98.45
5	−1	−1	1	85.42
6	1	−1	1	90.13
7	−1	1	1	90.75
8	1	1	1	99.70
9	−1.68	0	0	85.15
10	1.68	0	0	92.18
11	0	−1.68	0	75.55
12	0	1.68	0	99.52
13	0	0	−1.68	90.25
14	0	0	1.68	95.70
15	0	0	0	97.30
16	0	0	0	97.18
17	0	0	0	97.25

Table 4: Results of ANOVA for the fitted model.

Source	Degree of freedom	Sum of squares	Mean square	F value	P value
Model	9	1103.07	122.56	230.5	<0.0001
Residual	7	3.72	0.53		
Total	16	1106.7916			

Table 5: Correlation of model.

R^2	R^2_{adj}	Standard deviation	Mean	Coefficient of variation (%)
0.9966	0.9923	0.73	91.01	0.8

3.12. Evolution of Adsorption under Optimal Conditions. To confirm the validity of the theoretical values of the optimization, a follow-up of the evolution of the adsorption under the optimal conditions has been carried out (Figure 11). In this case, we notice that the system leads to a rapid adsorption of 98.91% after 5 min close to the theoretical value.

From what have been stated the above, CCD has shown great satisfaction in optimizing the parameters influencing the adsorption of the studied dyes mixture since the

Table 6: Estimated regression coefficients and their significance.

Coefficients	Estimated values	Standard deviation	F value	P value
b_0	97.22	0.42	230.5	<0.0001
b_1	1.83	0.2	85.95	<0.0001
b_2	7.22	0.2	1338.61	<0.0001
b_3	1.77	0.2	80.29	<0.0004
b_{11}	−2.95	0.22	184.92	0.0847
b_{22}	−3.35	0.22	238.34	0.0002
b_{33}	−1.43	0.22	43.32	<0.0001
b_{12}	0.52	0.26	4.03	<0.0001
b_{13}	1.77	0.26	47.14	<0.0001
b_{23}	−3.56	0.26	190.68	<0.0001

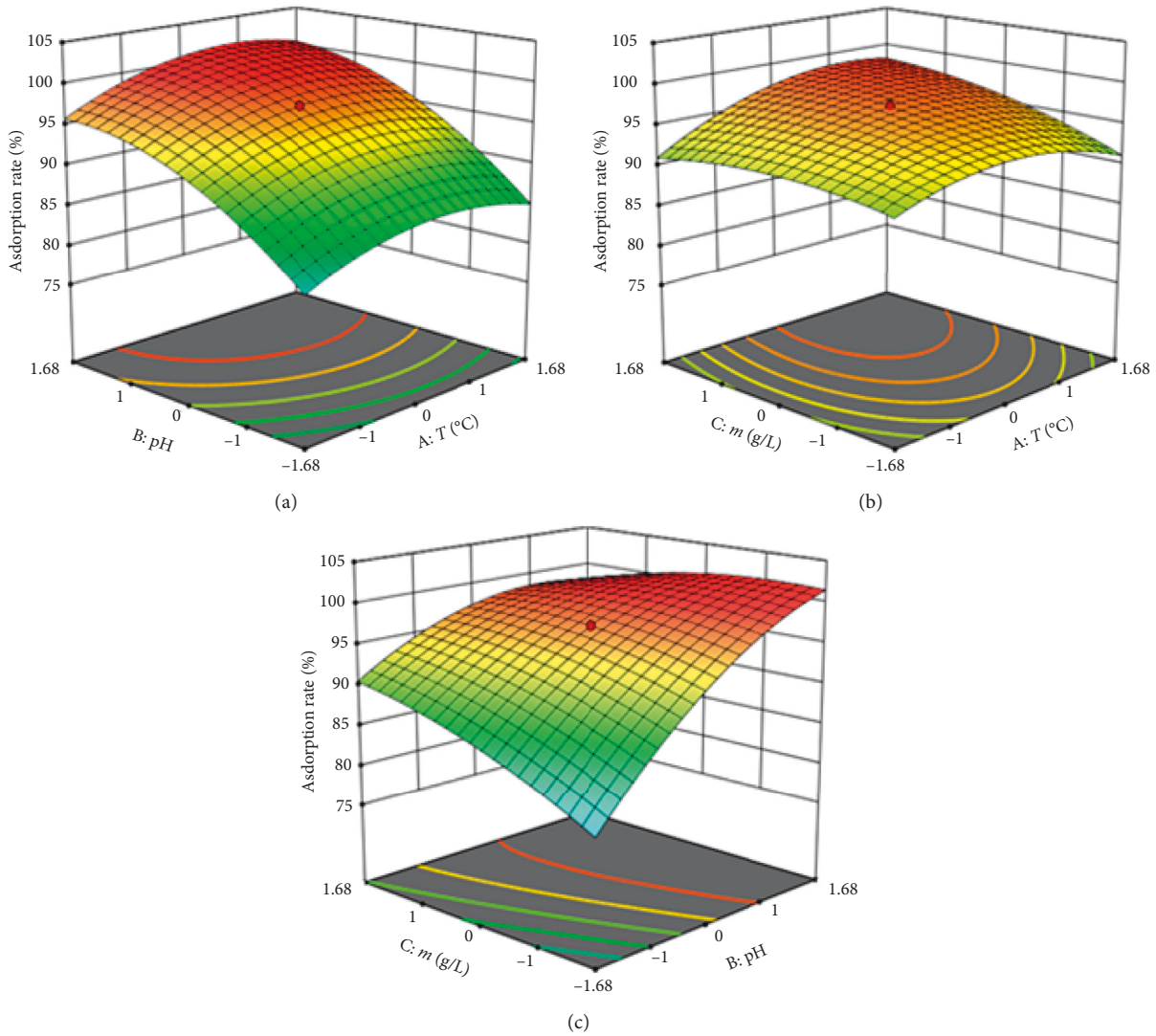

Figure 10: Response surfaces showing adsorption efficiency as function of (a) temperature and pH, (b) temperature and adsorbent dose, and (c) pH and adsorbent dose.

statistical tests are well adapted to the experimental results. These outcomes are in total agreement with the various publications, which show the validation of the CCD plane in the study of adsorption of dyes on different types of adsorbents [55–57]. In addition, the yield obtained at optimal conditions is very high, which confirms the performance of the pineapple bark as an adsorbent for the studied mixture.

Table 7: Established optimal conditions.

Optimal conditions			Adsorption (%)
Temperature (°C)	pH	Adsorbent dose ($g \cdot L^{-1}$)	
30	9.8	2.5	99.96

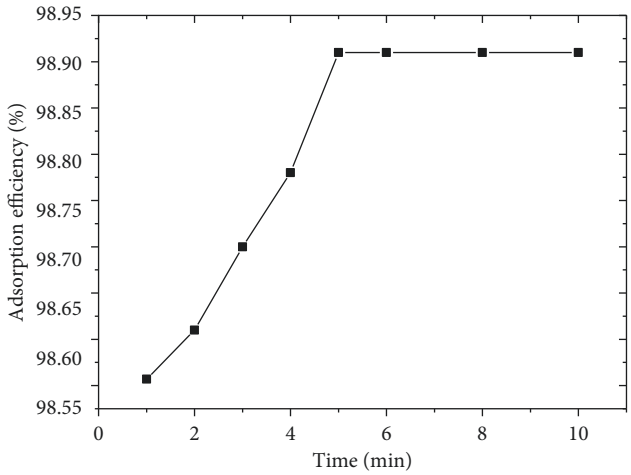

Figure 11: Evolution of the adsorption of DM under optimal conditions.

4. Conclusions

The performance of the pineapple bark in the adsorption of the dyes mixture Methylene Blue, Brilliant Green, and Congo Red has been studied in a batch system. In this respect, the parameters the mass of the adsorbent, the concentration of the dyes mixture, the pH, and the temperature have indeed influenced the adsorption process. Besides, adsorption at a concentration of 20 $mg \cdot L^{-1}$ is rapid during the first five minutes of contact for a mass of 2 $g \cdot L^{-1}$. Moreover, the adsorption is favorable in acidic medium and is of the exothermic type. Furthermore, through the experimental design methodology, CCD plan, we have optimized the physicochemical parameters such as the mass of the adsorbent, the pH, and the temperature influencing the adsorption of the dyes mixture into pineapple bark. During 5 min of the adsorption, under the optimum conditions pH = 9.8, $T = 30°C$, and adsorbent dose = 2.5 $g \cdot L^{-1}$, the output reaches 98.91% at an initial concentration of 20 $mg \cdot L^{-1}$ and for a volume of 50 mL.

Data Availability

No data were used to support this study.

Conflicts of Interest

The authors declare that they have no conflicts of interest.

Acknowledgments

The authors are grateful to the Laboratory of Biochemistry of the Faculty of Medicine and Pharmacy and the Innovation Center, Sidi Mohamed Ben Abdellah University of Fez (Morocco), for the financial support given to Dr. Ahlam Fegousse.

References

[1] A. El Gaidoumi, J. M. Doña-Rodríguez, E. Pulido Melián et al., "Mesoporous pyrophyllite-titania nanocomposites: synthesis and activity in phenol photocatalytic degradation," *Research on Chemical Intermediates*, vol. 45, no. 2, pp. 333–353, 2018.

[2] A. El Gaidoumi, J. M. Doña Rodríguez, E. Pulido Melián et al., "Synthesis of sol-gel pyrophyllite/TiO_2 heterostructures: effect of calcination temperature and methanol washing on photocatalytic activity," *Surfaces and Interfaces*, vol. 14, pp. 19–25, 2019.

[3] Y. Miyah, A. Lahrichi, M. Idrissi, A. Khalil, and F. Zerrouq, "Adsorption of methylene blue dye from aqueous solutions onto walnut shells powder: equilibrium and kinetic studies," *Surfaces and Interfaces*, vol. 11, pp. 74–81, 2018.

[4] Y. Miyah, M. Idrissi, and F. Zerrouq, "Study and modeling of the kinetics methylene blue adsorption on the clay adsorbents (Pyrophillite, Calcite)," *Journal of Materials and Environmental Sciences*, vol. 6, no. 3, pp. 699–712, 2015.

[5] M. Soni, A. K. Sharma, J. K. Srivastava, and J. S. Yadav, "Adsorptive removal of Methylene blue dye from an aqueous solution using water hyacinth root powder as a low cost adsorbent," *International Journal of Chemical Science and Applications*, vol. 3, no. 3, pp. 338–345, 2012.

[6] A. Bhatnagar and M. Sillanpää, "Utilization of agro-industrial and municipal waste materials as potential adsorbents for water treatment—a review," *Chemical Engineering Journal*, vol. 157, no. 2-3, pp. 277–296, 2010.

[7] G. Crini, "Non-conventional low-cost adsorbents for dye removal: a review," *Bioresource Technology*, vol. 97, no. 9, pp. 1061–1085, 2006.

[8] M. Rafatullah, O. Sulaiman, R. Hashim, and A. Ahmad, "Adsorption of methylene blue on low-cost adsorbents: a review," *Journal of Hazardous Materials*, vol. 177, no. 1–3, pp. 70–80, 2010.

[9] Y. Miyah, A. Lahrichi, M. Idrissi, S. Boujraf, H. Taouda, and F. Zerrouq, "Assessment of adsorption kinetics for removal potential of Crystal Violet dye from aqueous solutions using Moroccan pyrophyllite," *Journal of the Association of Arab Universities for Basic and Applied Sciences*, vol. 23, no. 1, pp. 20–28, 2018.

[10] Y. S. Al-Degs, M. A. M. Khraisheh, S. J. Allen, and M. N. Ahmad, "Adsorption characteristics of reactive dyes in columns of activated carbon," *Journal of Hazardous Materials*, vol. 165, no. 1–3, pp. 944–949, 2009.

[11] V. K. Gupta and Suhas, "Application of low-cost adsorbents for dye removal—a review," *Journal of Environmental Management*, vol. 90, no. 8, pp. 2313–2342, 2009.

[12] K. S. Bharathi and S. T. Ramesh, "Removal of dyes using agricultural waste as low-cost adsorbents: a review," *Applied Water Science*, vol. 3, no. 4, pp. 773–790, 2013.

[13] S. Agarwal, I. Tyagi, V. K. Gupta, N. Ghasemi, M. Shahivand, and M. Ghasemi, "Kinetics, equilibrium studies and thermodynamics of methylene blue adsorption on *Ephedra strobilacea* saw dust and modified using phosphoric acid and zinc chloride," *Journal of Molecular Liquids*, vol. 218, pp. 208–218, 2016.

[14] L. C. Morais, O. M. Freitas, E. P. Gonçalves, L. T. Vasconcelos, and C. G. González Beça, "Reactive dyes removal from wastewaters by adsorption on eucalyptus bark: variables that

define the process," *Water Research*, vol. 33, no. 4, pp. 979–988, 1999.

[15] R. Sivaraj, C. Namasivayam, and K. Kadirvelu, "Orange peel as an adsorbent in the removal of acid violet 17 (acid dye) from aqueous solutions," *Waste Management*, vol. 21, no. 1, pp. 105–110, 2001.

[16] S. Netpradit, P. Thiravetyan, and S. Towprayoon, "Application of 'waste' metal hydroxide sludge for adsorption of azo reactive dyes," *Water Research*, vol. 37, no. 4, pp. 763–772, 2003.

[17] S. Wang, Y. Boyjoo, A. Choueib, and Z. H. Zhu, "Removal of dyes from aqueous solution using fly ash and red mud," *Water Research*, vol. 39, no. 1, pp. 129–138, 2005.

[18] D. Mohan, K. P. Singh, G. Singh, and K. Kumar, "Removal of dyes from wastewater using flyash, a low-cost adsorbent†," *Industrial & Engineering Chemistry Research*, vol. 41, no. 15, pp. 3688–3695, 2002.

[19] A. Espantaleón, J. A. Nieto, M. Fernandez, and A. Marsal, "Use of activated clays in the removal of dyes and surfactants from tannery waste waters," *Applied Clay Science*, vol. 24, no. 1-2, pp. 105–110, 2003.

[20] S. Hashemian and M. R. Shahedi, "Novel Ag/Kaolin nanocomposite as adsorbent for removal of acid cyanine 5R from aqueous solution," *Journal of Chemistry*, vol. 2013, Article ID 285671, 7 pages, 2013.

[21] S. Tetteh, A. Quashie, and M. Akrofi Anang, "Purification, characterization, and time-dependent adsorption studies of Ghanaian muscovite clay," *Journal of Chemistry*, vol. 2018, Article ID 6252913, 8 pages, 2018.

[22] B. H. Dang Son, V. Q. Mai, D. X. Du, N. H. Phong, and D. Q. Khieu, "A study on astrazon black AFDL dye adsorption onto vietnamese diatomite," *Journal of Chemistry*, vol. 2016, Article ID 8685437, 11 pages, 2016.

[23] M. A. Al-Ghouti, M. A. M. Khraisheh, S. J. Allen, and M. N. Ahmad, "The removal of dyes from textile wastewater: a study of the physical characteristics and adsorption mechanisms of diatomaceous earth," *Journal of Environmental Management*, vol. 69, no. 3, pp. 229–238, 2003.

[24] O. Ozdemir, B. Armagan, M. Turan, and M. S. Çelik, "Comparison of the adsorption characteristics of azo-reactive dyes on mezoporous minerals," *Dyes and Pigments*, vol. 62, no. 1, pp. 49–60, 2004.

[25] B. Armagan, M. Turan, and M. S. Celik, "Equilibrium studies on the adsorption of reactive azo dyes into zeolite," *Desalination*, vol. 170, no. 1, pp. 33–39, 2004.

[26] A. Krysztafkiewicz, S. Binkowski, and T. Jesionowski, "Adsorption of dyes on a silica surface," *Applied Surface Science*, vol. 199, no. 1–4, pp. 31–39, 2002.

[27] M. Özacar and I. Ayhan Sengil, "Adsorption of acid dyes from aqueous solutions by calcined alunite and granular activated carbon," *Adsorption*, vol. 8, no. 4, pp. 301–308, 2002.

[28] Y. C. Wong, Y. S. Szeto, W. H. Cheung, and G. McKay, "Adsorption of acid dyes on chitosan—equilibrium isotherm analyses," *Process Biochemistry*, vol. 39, no. 6, pp. 693–702, 2004.

[29] S. J. Allen, G. Mckay, and J. F. Porter, "Adsorption isotherm models for basic dye adsorption by peat in single and binary component systems," *Journal of Colloid and Interface Science*, vol. 280, no. 2, pp. 322–333, 2004.

[30] Z. Aksu and S. Tezer, "Biosorption of reactive dyes on the green alga *Chlorella vulgaris*," *Process Biochemistry*, vol. 40, no. 3-4, pp. 1347–1361, 2005.

[31] T. O'Mahony, E. Guibal, and J. M. Tobin, "Reactive dye biosorption by Rhizopusarrhizus biomass," *Enzyme and Microbial Technology*, vol. 31, no. 4, pp. 456–463, 2002.

[32] G. Crini, "Studies on adsorption of dyes on beta-cyclodextrin polymer," *Bioresource Technology*, vol. 90, no. 2, pp. 193–198, 2003.

[33] G. Crini and M. Morcellet, "Synthesis and applications of adsorbents containing cyclodextrins," *Journal of Separation Science*, vol. 25, no. 13, pp. 1–25, 2002.

[34] F. Delval, G. Crini, J. Vebrel, M. Knorr, G. Sauvin, and E. Conte, "Starch-modified filters used for the removal of dyes from waste water," *Macromolecular Symposia*, vol. 203, no. 1, pp. 165–172, 2003.

[35] I. Bouzaida and M. B. Rammah, "Adsorption of acid dyes on treated cotton in a continuous system," *Materials Science and Engineering: C*, vol. 21, no. 1-2, pp. 151–155, 2002.

[36] J. Rivera-Utrilla, I. Bautista-Toledo, M. A. Ferro-García, and C. Moreno-Castilla, "Activated carbon surface modifications by adsorption of bacteria and their effect on aqueous lead adsorption," *Journal of Chemical Technology & Biotechnology*, vol. 76, no. 12, pp. 1209–1215, 2001.

[37] Y. Miyah, A. Lahrichi, and M. Idrissi, "Removal of cationic dye-methylene blue-from aqueous solution by adsorption onto corn cob powder calcined," *Journal of Materials and Environmental Science*, vol. 7, no. 1, pp. 96–104, 2016.

[38] A. Fegousse, Y. Miyah, R. Elmountassir, and A. Lahrichi, "Valorization of pineapple bark for removal of a cationic dye sush as methylene blue," *Journal of Materials and Environmental Science*, vol. 9, no. 8, pp. 2449–2457, 2018.

[39] A. K. Rana, R. K. Basak, B. C. Mitra, M. Lawther, and A. N. Banerjee, "Studies of acetylation of jute using simplified procedure and its characterization," *Journal of Applied Polymer Science*, vol. 64, no. 8, pp. 1517–1523, 1997.

[40] N. Wibowo, L. Setyadhi, D. Wibowo, J. Setiawan, and S. Ismadji, "Adsorption of benzene and toluene from aqueous solutions onto activated carbon and its acid and heat treated forms: influence of surface chemistry on adsorption," *Journal of Hazardous Materials*, vol. 146, no. 1-2, pp. 237–242, 2007.

[41] M. El Haddad, R. Mamouni, N. Saffaj, and S. Lazar, "Removal of a cationic dye–basic Red 12–from aqueous solution by adsorption onto animal bone meal," *Journal of the Association of Arab Universities for Basic and Applied Sciences*, vol. 12, no. 1, pp. 48–54, 2018.

[42] W.-T. Tsai, H.-C. Hsu, T.-Y. Su, K.-Y. Lin, C.-M. Lin, and T.-H. Dai, "The adsorption of cationic dye from aqueous solution onto acid-activated andesite," *Journal of Hazardous Materials*, vol. 147, no. 3, pp. 1056–1062, 2007.

[43] C.-H. Weng and Y.-F. Pan, "Adsorption of a cationic dye (methylene blue) onto spent activated clay," *Journal of Hazardous Materials*, vol. 144, no. 1-2, pp. 355–362, 2007.

[44] A. R. Dinçer, Y. Guner, and N. Karakaya, "Coal-based bottom ash (CBBA) waste material adsorbent for removal of textile dyestuffs from aqueous solution," *Journal of Hazardous Materials*, vol. 141, no. 3, pp. 529–535, 2006.

[45] A. El Gaidoumi, A. Chaouni Benabdallah, A. Lahrichi, and A. Kherbeche, "Adsorption of phenol in aqueous medium by a raw and treated moroccan pyrophyllite," *Journal of Materials and Environmental Science*, vol. 6, pp. 2247–2259, 2015.

[46] A. El Gaidoumi, J. M. Doña-Rodríguez, E. Pulido Melián et al., "Catalytic efficiency of Cu-supported pyrophyllite in heterogeneous catalytic oxidation of phenol," *Arabian Journal for Science and Engineering*, 2019.

[47] A. El Gaidoumi, A. Loqman, A. C. Benadallah, B. El Bali, and A. Kherbeche, "Co(II)-pyrophyllite as catalyst for phenol oxidative degradation: optimization study using response surface methodology," *Waste and Biomass Valorization*, pp. 1–9, 2017.

[48] O. B. Ayodele, J. K. Lim, and B. H. Hameed, "Degradation of phenol in photo-fenton process by phosphoric acid modified kaolin supported ferric-oxalate catalyst: optimization and kinetic modeling," *Chemical Engineering Journal*, vol. 197, pp. 181–192, 2012.

[49] H. Li, Y. Li, L. Xiang et al., "Heterogeneous photo-fenton decolorization of orange II over Al-pillared Fe-smectite: response surface approach, degradation pathway, and toxicity evaluation," *Journal of Hazardous Materials*, vol. 287, pp. 32–41, 2015.

[50] L. C. Almeida, S. Garcia-Segura, N. Bocchi, and E. Brillas, "Solar photoelectro-fenton degradation of paracetamol using a flow plant with a Pt/air-diffusion cell coupled with a compound parabolic collector: process optimization by response surface methodology," *Applied Catalysis B: Environmental*, vol. 103, no. 1-2, pp. 21–30, 2011.

[51] J. Herney-Ramirez, M. Lampinen, M. A. Vicente, C. A. Costa, and L. M. Madeira, "Experimental design to optimize the oxidation of orange II dye solution using a clay-based fenton-like catalyst," *Industrial & Engineering Chemistry Research*, vol. 47, no. 2, pp. 284–294, 2008.

[52] F. Torrades and J. García-Montaño, "Using central composite experimental design to optimize the degradation of real dye wastewater by fenton and photo-fenton reactions," *Dyes and Pigments*, vol. 100, pp. 184–189, 2014.

[53] A. Long, H. Zhang, and Y. Lei, "Surfactant flushing remediation of toluene contaminated soil: optimization with response surface methodology and surfactant recovery by selective oxidation with sulfate radicals," *Separation and Purification Technology*, vol. 118, pp. 612–619, 2013.

[54] I. Arslan-Alaton, G. Tureli, and T. Olmez-Hanci, "Optimization of the photo-Fenton-like process for real and synthetic azo dye production wastewater treatment using response surface methodology," *Photochemical & Photobiological Sciences*, vol. 8, no. 5, pp. 628–638, 2009.

[55] J. Sharma, Sukriti, P. Anand et al., "RSM-CCD optimized adsorbent for the sequestration of carcinogenic rhodamine-B: kinetics and equilibrium studies," *Materials Chemistry and Physics*, vol. 196, pp. 270–283, 2017.

[56] J. S. Sukriti, J. Sharma, A. S. Chadha et al., "Sequestration of dyes from artificially prepared textile effluent using RSM-CCD optimized hybrid backbone based adsorbent-kinetic and equilibrium studies," *Journal of Environmental Management*, vol. 190, pp. 176–187, 2017.

[57] Z. Anfar, R. El Haouti, S. Lhanafi, M. Benafqir, Y. Azougarh, and N. El Alem, "Treated digested residue during anaerobic co-digestion of Agri-food organic waste: methylene blue adsorption, mechanism and CCD-RSM design," *Journal of Environmental Chemical Engineering*, vol. 5, no. 6, pp. 5857–5867, 2017.